

# Chlorine-resistant positively charged nanofiltration membranes formed by SI-ATRP method for heavy metal ions removal

Bin Wu<sup>1</sup>, Xiao-Dan Weng<sup>2</sup>, Naixin Wang<sup>1</sup>, Ming-Jie Yin<sup>1</sup>, Lin Zhang<sup>2</sup>, and Quan-Fu An<sup>1</sup>

<sup>1</sup>Beijing University of Technology

<sup>2</sup>Zhejiang University

March 30, 2022

## Abstract

Heavy metal pollution is one of the most serious environmental problems. Nanofiltration is an effective and potential membrane separation technology for removal of heavy metal ions from water. However, the separation performance and chlorine resistance of the nanofiltration membrane should be further improved in industry. In this study, positively charged polyamide (PA-PDMC) nanofiltration membranes were fabricated to remove heavy metal ions from water. The obtained membrane had high flux and chlorine resistance by grafting methacryloxyethyltrimethyl ammonium chloride (DMC) on the surface of 2-bromoisobutyryl bromide (BIBB) immobilized polyamide (PA-Br1) membranes via surface-initiated atom transfer radical polymerization (SI-ATRP). The retentions to divalent cations of the as-prepared PA-PDMC membrane was above 90% with the flux of 82.5 L m<sup>-2</sup> h<sup>-1</sup>. Furthermore, the PA-PDMC membrane showed a stable separation performance during a long-time filtration process of 168 h, which exhibited an exceptional chlorine resistance.

## Chlorine-resistant positively charged nanofiltration membranes formed by SI-ATRP method for heavy metal ions removal

Bin Wu<sup>a</sup>, Xiao-Dan Weng<sup>b</sup>, Naixin Wang<sup>a\*</sup>, Ming-Jie Yin<sup>a</sup>, Lin Zhang<sup>b</sup>, Quan-Fu An<sup>a11\*</sup> Corresponding authors. E-mail: wangnx@bjut.edu.cn (N. Wang), anqf@bjut.edu.cn (Q. An)

<sup>a</sup> Beijing Key Laboratory for Green Catalysis and Separation, Department of Environmental Chemical Engineering, Beijing University of Technology, Beijing 100124, China.

<sup>b</sup> Engineering Research Center of Membrane and Water Treatment of MOE, College of Chemical and Biological Engineering, Zhejiang University, Hangzhou 310027, China.

**ABSTRACT:** Heavy metal pollution is one of the most serious environmental problems. Nanofiltration is an effective and potential membrane separation technology for removal of heavy metal ions from water. However, the separation performance and chlorine resistance of the nanofiltration membrane should be further improved in industry. In this study, positively charged polyamide (PA-PDMC) nanofiltration membranes were fabricated to remove heavy metal ions from water. The obtained membrane had high flux and chlorine resistance by grafting methacryloxyethyltrimethyl ammonium chloride (DMC) on the surface of 2-bromoisobutyryl bromide (BIBB) immobilized polyamide (PA-Br1) membranes via surface-initiated atom transfer radical polymerization (SI-ATRP). The retentions to divalent cations of the as-prepared PA-PDMC membrane was above 90% with the flux of 82.5 L m<sup>-2</sup> h<sup>-1</sup>. Furthermore, the PA-PDMC membrane showed a stable separation performance during a long-time filtration process of 168 h, which exhibited an exceptional chlorine resistance.

**KEYWORDS:** methacryloxyethyltrimethyl ammonium chloride; surface-initiated atom transfer radical polymerization; positively charged membrane; high flux; chlorine resistance

## 1. INTRODUCTION

Heavy metal ions separation is a crucial procedure for industrial wastewater treatment.<sup>1,2</sup> Among various separation methods, membrane technology is emerging as a promising resolution to address this challenge because of their energy efficiency and environmental-friendly.<sup>3</sup> Given the size and charge property of heavy metal ions, nanofiltration membranes are suitable due to its synergetic separation mechanisms involving steric hindrance effect and electrostatic repulsive effect.<sup>4-6</sup> Nowadays, polyamide thin film composite membranes fabricated by interfacial polymerization have experienced significant progress, which was regarded as the state-of-the-art technology to prepare nanofiltration membrane.<sup>7,8</sup> However, most commercially polyamide nanofiltration membranes are negatively charged and unsuitable for water softening and heavy metal ions removal.<sup>9,10</sup> On the other hand, membrane fouling especially biofouling is an inevitable problem during the practical application process.<sup>11</sup> To minimize the influence of fouling on a membrane, chlorine or other oxidants were added to the feed, which may also result in degradation of polyamide membranes associated with performance deterioration.<sup>12,13</sup> For prolong the life of polyamide thin film composite membranes, two novel zwitterionic amide monomers were synthesized to prepare antifouling polyamide nanofiltration membranes in which the hydration layer built by zwitterionic group resulted in outstanding anti-adhesion performance toward bacteria and protein.<sup>14,15</sup> Meanwhile, constructing zwitterionic top layer by surface grafting to polyamide active layer can also effectively improve the anti-fouling property of membranes.<sup>16-18</sup> Moreover, tetrakis(hydroxymethyl) phosphonium chloride (THPC) was exploited in surface modification of polyamide nanofiltration membranes which were endowed with powerful capacity to destroy a series of microorganisms and extremely high water permeability.<sup>19</sup> Besides, improving the stability of polyamide membranes in the presence of active chlorine is another efficient method. Hence, there is an intense need for fabricating positively charged polyamide membranes with high separation performance and strong chlorine resistance.<sup>20</sup>

Currently, great efforts have been taken to fabricate positively charged polyamide nanofiltration membranes. For example, Ruaan et al.<sup>21</sup> selected hyperbranched polyethyleneimine (PEI) as polyamine monomers to prepare positively charged polyamide nanofiltration membranes by interfacial polymerization. The water permeability and retention to  $MgCl_2$  of the membranes were  $9.5 \text{ L m}^{-2} \text{ h}^{-1} \text{ bar}^{-1}$  and 80%, respectively. For the further enhancement of membrane performance, poly(dopamine) modified multiwall carbon nanotubes were embedded in PEI.<sup>22</sup> The water permeability and retention to  $MgCl_2$  were both improved, which reached to  $15.3 \text{ L m}^{-2} \text{ h}^{-1} \text{ bar}^{-1}$  and 91.5%, respectively. Positively charged nanofiltration polyamide nanofiltration membranes were also fabricated by changing the organic solvent in the process of interfacial polymerization. The resulting rejection to  $CaCl_2$  achieved 95.1% with the flux of  $12.7 \text{ L m}^{-2} \text{ h}^{-1} \text{ bar}^{-1}$ , which resulted from the enhancement of diffusion rate and solubility for piperazine (PIP).<sup>23</sup> Besides, surface modification has proved to be another effective method for building positively charged nanofiltration membrane. For instance, PEI was used to modify polyamide membranes through grafting techniques.<sup>24</sup> Chung et al.<sup>25</sup> fabricated surface-modified positively charged polyamide nanofiltration membranes by grafting poly(amidoamine) dendrimer on the surface of m-phenylenediamine/trimesoyl chloride hollow fiber membranes for heavy metal ions removal. The retentions to most divalent cations of the membranes were as high as 99% with the water permeability of  $3.6 \text{ L m}^{-2} \text{ h}^{-1} \text{ bar}^{-1}$ . These membranes exhibited excellent separation performance for divalent cations. However, all of these positively charged polyamide nanofiltration membranes contained amide groups, which would be oxidized when active chlorine was present. It resulted in significant performance degradation of polyamide membranes and therefore decreased the lifetime of the membranes.<sup>13</sup> Up to now, tertiary amide bonds has been demonstrated to possess obvious stability in the presence of oxidants.<sup>26,27</sup> Therefore, the substitution of tertiary amide for secondary amide in terms of polyamide membrane is one of the effective methods to optimize chlorine resistance. On the other hand, protective or sacrificial layers were constructed by surface modification of polyamide membrane to resist the attack of active chlorine effectively.<sup>28-30</sup> However, because of chemical cross-linking and chain transfer in free radical polymerization, the thickness of the surface modification layers was increased to reduce the water flux.<sup>31</sup> Therefore, another challenge in surface modification of polyamide nanofiltration membranes is to introduce positively charged groups in the separation layer without sacrificing water flux.<sup>32</sup>

Surface-initiated atom transfer radical polymerization (SI-ATRP) is a “living” radical polymerization pro-

cess, which can precisely control the graft length and density of polymers on the membrane surface.<sup>33</sup> Compared with other surface modifications, the SI-ATRP process reduces chain transfer and inhibits cross-linking of surface modification layers, which is a benefit for maintaining high water flux. In this study, 2-bromoisobutyryl bromide (BIBB)-immobilized polyamide (PA-Br1) membranes were prepared with PIP, TMC, and BIBB through interfacial polymerization. Subsequently, positively charged polyamide (PA-PDMC) thin film composite nanofiltration membranes with high flux and chlorine resistance were prepared through SI-ATRP. The structure, chemical property and separation performance of the membranes can be adjusted by varying the ATRP time. This work will be helpful to explore membranes with high flux and chlorine resistance for heavy metal ions removal.

## 2. EXPERIMENTAL SECTION

### 2.1. Materials.

Piperazine (PIP, 99%), trimesoyl chloride (TMC, 98%) and methacryloxyethyltrimethyl ammonium chloride (DMC, 80% aqueous solution) were purchased from TCI (Shanghai) Development Co., Ltd. Sodium hydroxide (NaOH, 96%), sodium hypochlorite (NaClO, active chlorine concentration 5.2%), sodium sulfate (Na<sub>2</sub>SO<sub>4</sub>, 99%), sodium chloride (NaCl, 99.5%), magnesium sulfate (MgSO<sub>4</sub>, 98%), magnesium chloride (MgCl<sub>2</sub>, 98%), calcium chloride (CaCl<sub>2</sub>, 96%), copper chloride (CuCl<sub>2</sub>, 99%), zinc chloride (ZnCl<sub>2</sub>, 98%), polyethylene glycol (PEG, molecular weight 200, 300, 400, 600, 800 and 1000 Da), hexane (97%) and methanol (99.7%) were obtained from Sinopharm Chemical Reagent Co., Ltd., Shanghai, China. 2-Bromoisobutyryl bromide (BIBB, 98%), 2, 2'-bipyridyl (BPY, 99%), copper (II) bromide (CuBr<sub>2</sub>, 99%), copper (I) bromide (CuBr, 99.999%), and poly(ethyleneimine) (PEI, 50% aqueous solution, molecular weight 10 kDa), were obtained from Sigma-Aldrich Co., Ltd. All the materials were used as received without any further purification. Deionized water (18 MΩ cm) was used in all experiments. Polysulfone ultrafiltration supporting membranes (PSF-UF, molecular weight cut-off 20 kDa) were kindly provided by the Development Centre of Water Treatment Technology, Hangzhou, China.

### 2.2. Preparation of PA-Br membranes.

As shown in Figure 1, the PA-Br membranes were prepared by interfacial polymerization of bromopolyamide onto the PSF-UF membrane. The PSF-UF membrane was immersed in an aqueous phase containing 0.35 wt% PIP and 0.01 mol L<sup>-1</sup> NaOH for 5 min. Then, the excess solution was removed from the membrane surface. Subsequently, the PIP-saturated support membrane was immersed in the hexane phase containing 0.20 wt% TMC and BIBB for 2 min to form the ultrathin bromopolyamide selective layer. After removing the excess organic solution, the resulting membrane was cured at 60 °C for 10 min. Finally, the prepared PA-Br membranes were washed thoroughly with methanol and water. The PA-Br membranes were stored in a cool, dark place in 50 vol% methanol-water which was replaced weekly to prevent bacteria breeding. As the chemical structure of PA-Br shown in Figure 1, the cross-linking, linear, and end extent of PA-Br membrane was denoted by x, y, and z, respectively. Herein, BIBB concentration in hexane was selected as 1.00 wt% to achieve an optimal separation performance in terms of both flux and retention.<sup>17</sup> The corresponding membrane was named as PA-Br1.

### 2.3. Preparation of PA-PDMC membranes.

The PA-PDMC membranes were prepared by SI-ATRP of DMC on the surface of PA-Br1 membranes (Figure 1). Firstly, three pieces of PA-Br1 membranes were placed into a flask under nitrogen protection. 40 mmol DMC, 12 mmol BPY, 1 mmol CuBr<sub>2</sub>, and 5 mmol CuBr were first dissolved in 125 mL 50 vol% methanol-water and the solution was then transferred into the flask after being purged with nitrogen for 30 min. Then, the reaction mixture in the flask was stirred at room temperature for a predetermined time (ATRP time). The reaction was terminated by exposing the mixture to air. Finally, the prepared PA-PDMC membranes were washed thoroughly with methanol and water. The PA-PDMC membranes were stored in a cool, dark place in 50 vol% methanol-water which was replaced weekly to prevent bacteria breeding. Herein, the corresponding membranes were named as PA-PDMC<sub>t</sub> membranes, where *t* represents the ATRP time (0.2, 0.5, 1.0, 3.0, and 8.0 h). To compare with the PA-PDMC membranes, the control membrane denoted

by PA was generated with PIP and TMC by the same interfacial polymerization process. The concentration of PIP and TMC was selected as 0.35 wt% and 0.2 wt% to achieve a good separation performance according to our previous study.<sup>14,34</sup>

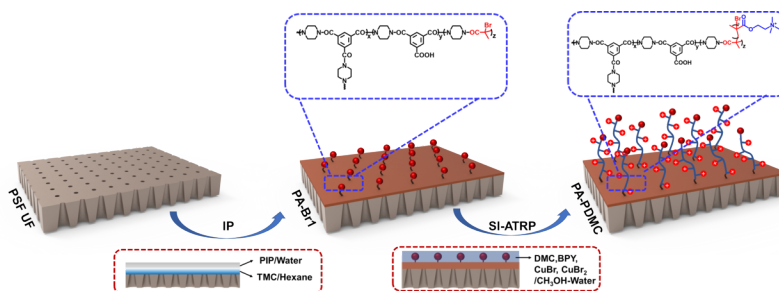


**Figure 1.** Synthetic scheme for preparing PA-PDMC membrane via interfacial polymerization (PIP/water concentration = 0.35 wt%, water solution additives: 0.01 mol L<sup>-1</sup> NaOH, TMC/hexane concentration = 0.20 wt%, reaction time = 2 min, cured at 60 °C for 10 min) and subsequently surface-initiated atom transfer radical polymerization (DMC: 40 mmol, BPY: 12 mmol; CH<sub>3</sub>OH-Water (V/V = 1): 125 mL, CuBr<sub>2</sub>: 1 mmol, CuBr: 5 mmol).

#### 2.4. Membrane characterization.

All the membrane samples were flushed with water and dried thoroughly at 25 °C under vacuum for 24 h prior to characterization. Chemical structures of membranes were characterized by attenuated total reflectance Fourier transform infrared spectroscopy (ATR-FTIR, Nicolet 6700, Thermo Fisher Scientific, USA) with a Ge crystal as the internal reflection element with an angle of incidence of 45°. Atomic compositions of membrane surface were determined by X-ray photoelectron spectroscopy (XPS, Escalab 250Xi, Thermo Fisher Scientific, USA). All binding energies were referred to the C (1s) peak at 284.6 eV.<sup>35</sup> The Zeta potential of membranes was characterized by an electrokinetic analyzer (SurPass, Anton Paar GmbH, Austria). The Zeta potential test was conducted with 1.0 mmol L<sup>-1</sup> KCl aqueous solutions at 25 °C and pH ranging from 3.0 to 10.0. Surface Zeta potential was determined from streaming current data using the Helmholtz-Smoluchowski equation. The data presented are the average values of the four tests. The cross-section and surface morphology of membranes were characterized by field emission scanning electron microscopy (FESEM, S4800, HITACHI, Japan). Membranes were fractured in liquid nitrogen to examine their cross-section structures. SEM samples were sputter-coated with gold and analyzed at a voltage of 3 kV. Membrane surface roughness was analyzed using multimode atomic force microscopy (AFM, SPI3800N, Seiko Instruments Inc., Japan) in tapping mode at room temperature in the air atmosphere. The surface roughness of each membrane was quantified in terms of the measured root mean square (RMS) roughness. The surface hydrophilicity of membranes was evaluated from dynamic water contact angle measurements (OCA 20, Data Physics Instruments GmbH, Germany) using the sessile drop method at ambient temperature. The highest and the lowest equilibrium angles tested in five random locations were discarded and the remaining data were averaged.

#### 2.5. Nanofiltration performance.

Water flux and solute retention of PA-PDMC membranes were investigated with a cross-flow nanofiltration apparatus (Figure 2). The membranes were pre-filtrated with water at 25 °C and 0.6 MPa to reach a steady-state before testing. Then the solute retention was measured with PEG and inorganic salts aqueous solution respectively. The permeate was reclaimed to keep the concentration of the feed. Between each different feed solution test or after completing the tests, the membranes were rinsed thoroughly with water. The water flux ( $J$ ) and solute retention ( $R$ ) were calculated by the following Eqs. (1) and Eqs. (2):

$$J = \frac{V}{A \cdot t} \quad (1)$$

$$R = \left(1 - \frac{C_P}{C_F}\right) \times 100\% \quad (2)$$

where  $V$  (L) is the volume of permeation over a time interval  $\Delta t$  (h),  $A$  is the effective area of the membrane ( $22.4 \text{ cm}^2$ ),  $C_P$  and  $C_F$  ( $\text{g L}^{-1}$ ) are the solute concentrations of the permeate and feed, respectively. The solute concentrations were determined from conductivity (FE30, Mettler-Toledo, Switzerland) for inorganic salts or total organic carbon analysis (TOC-L, Shimadzu, Japan) for PEG. Each membrane was examined at least three times and the average was recorded as the result.

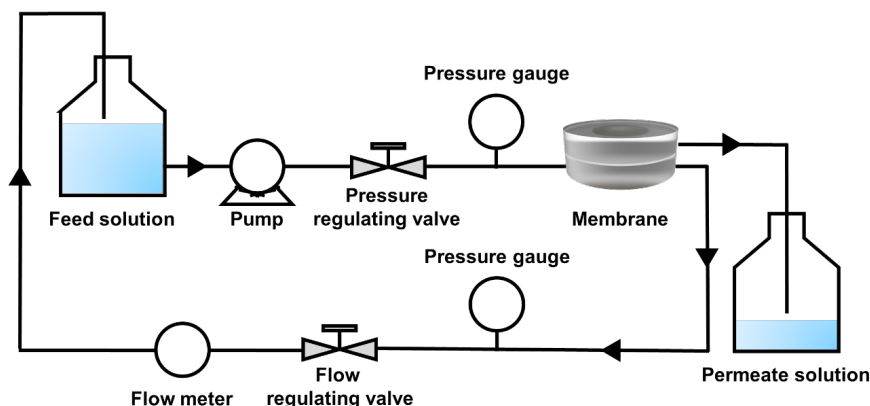


**Figure 2.** Schematic illustration of a cross-flow nanofiltration apparatus.

### 3. RESULTS AND DISCUSSION

#### 3.1. Chemical structures of PA-PDMC membranes.

Figure 3(a) presents ATR-FTIR spectra in the wavenumber range of  $900\text{--}2100 \text{ cm}^{-1}$  of the PA-Br1 membrane and PA-PDMC membranes grafted via SI-ATRP for a different time. For the spectrum of PA-Br1 membrane, the characteristic peaks appearing at  $1621$ ,  $1242$ , and  $1106 \text{ cm}^{-1}$  are assigned to stretching vibrations of the amide carbonyl ( $-\text{CON}<$ ) of bromopolyamide and sulfone group ( $\text{O}=\text{S}=\text{O}$ ) on the PSF-UF support membrane. After grafting PDMC on the surface of the PA-Br1 membrane, new peaks at  $1726$  and  $955 \text{ cm}^{-1}$  appeared in the spectrum of the PA-PDMC membrane, which were characteristic peaks of the ester carbonyl ( $-\text{COO}-$ ) and quaternary ammonium group ( $>\text{N}^+(\text{CH}_3)_2$ ) on DMC, respectively. Moreover, for the spectra of the PA-PDMC membrane, the intensity of ester carbonyl ( $1726 \text{ cm}^{-1}$ ) increases with increasing the ATRP time from  $0.2$  to  $8.0 \text{ h}$ . Since the depth of the reflected IR beam in the ATR-FTIR technique is typically somewhat below  $1 \mu\text{m}$ , the peaks of the PSF-UF support are visible after interfacial polymerization and SI-ATRP indicates that the selective layer of PA-PDMC membrane is thinner than  $1 \mu\text{m}$ .<sup>36</sup> Furthermore, the N1s core-level XPS spectra of the PA-Br1 and PA-PDMC membranes were also collected. As shown in Figure 3(b), for the N1s core-level XPS spectrum of PA-Br1 membrane, the emission peaks appearing at  $399.3 \text{ eV}$  are assigned as the binding energy of N1s of amide groups. After grafting PDMC on the surface of the PA-Br1 membrane, the spectra of the PA-PDMC membrane shows the appearance of emission peaks at  $402.0 \text{ eV}$ , which is the characteristic peak of the binding energy of  $\text{N}^+1\text{s}$  of quaternary ammonium groups. Meanwhile, the intensity of  $\text{N}^+1\text{s}$  increases with increasing the ATRP time from  $0.2$  to  $8.0 \text{ h}$ . Therefore, all of these results demonstrate that PDMC was grafted on the surface of the PA-Br1 membrane via SI-ATRP, and the DMC content on the membrane surface increases with increasing the ATRP time.

#### Hosted file

image3.emf available at <https://authorea.com/users/469418/articles/562301-chlorine-resistant-positively-charged-nanofiltration-membranes-formed-by-si-atrp-method-for-heavy-metal-ions-removal>

**Figure 3.** (a) ATR-FTIR spectra and (b) N1s core-level XPS spectra of PA-Br1 and PA-PDMC membrane grafted via SI-ATRP for different time.

### 3.2. Surface and cross-section characterization of PA-PDMC membrane.

Apart from the chemical structures, the membrane morphologies were also changed after performing SI-ATRP of DMC from the membrane surface. Figure 4 presents the surface morphologies of the PA-Br1 and PA-PDMC membranes. The SEM and AFM images of PA-Br1 membrane surface (Figure 4(a)) show a nodular morphology with an RMS value of 27.3 nm. However, the surface morphologies for the PA-PDMC membrane are different, which exhibit a pancake morphology.<sup>37</sup> As the ATRP time increases from 0.2 to 8.0 h, the RMS value of the PA-PDMC membrane increases from 33.1 to 157.6 nm ((Figure 4(b)-(f)).

Furthermore, an increasing variation on the selective layer thickness of the PA-PDMC membrane was also characterized by SEM (Figure 5). As shown in Figure 5(a), the thickness of bromopolyamide selective layer on the PA-Br1 membrane is about 190 nm. The thickness of the PA-PDMC membrane increases from 210 to 450 nm with increasing the ATRP time from 0.2 to 8.0 h ((Figure 5(b)-(f)). The differences in surface morphologies and selective layer thickness between PA-Br1 and PA-PDMC membranes are probably ascribed to the PDMC layer grafted on the PA-Br1 membrane. As far as we know, SI-ATRP is a “living” process. The degree of polymerization and graft content of PDMC chains on the PA-Br1 membrane increases with increasing the ATRP time over the whole SI-ATRP process, resulting in an obvious pancake morphology and an increase in the selective layer thickness.<sup>38,39</sup>

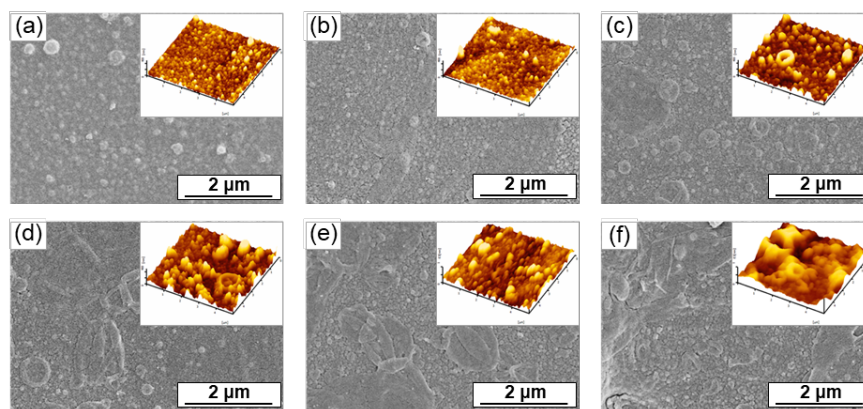


**Figure 4.** SEM ( $\times 20.0k$ )/AFM images of different membranes: (a) PA-Br1 (RMS=27.3), (b) PA-PDMC0.2 (RMS=33.1), (c) PA-PDMC0.5 (RMS=56.1), (d) PA-PDMC1 (RMS=71.8), (e) PA-PDMC3 (RMS=104.7) and (f) PA-PDMC8 (RMS=157.6).

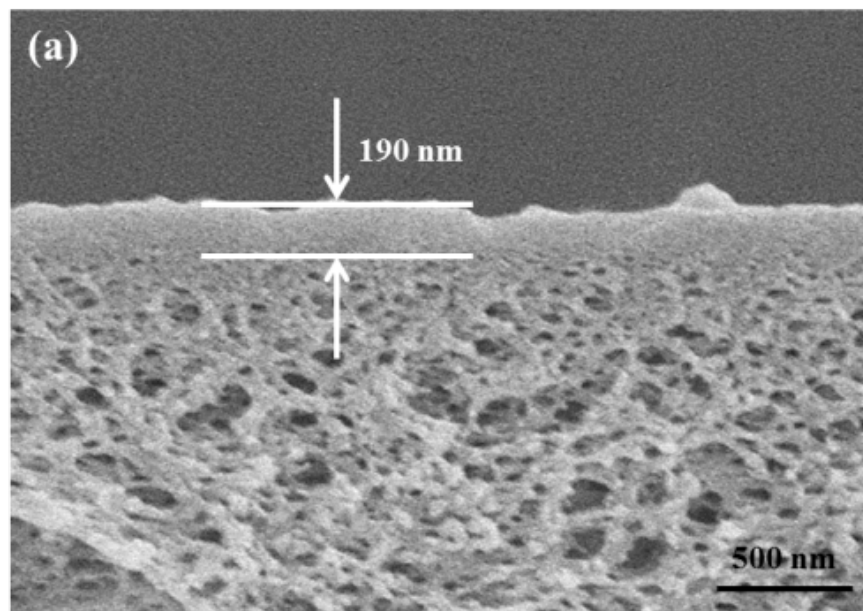


**Figure 5.** Cross-section ( $\times 40.0k$ ) morphologies of different membranes: (a) PA-Br1, (b) PA-PDMC0.2, (c) PA-PDMC0.5, (d) PA-PDMC1, (e) PA-PDMC3 and (f) PA-PDMC8.

The water contact angle (WCA) was used to investigate the hydrophilicity of PA-Br1 and PA-PDMC membranes. As shown in Figure 6(a), the WCA of the PA-Br1 membrane is  $56.8^\circ$ . After grafting PDMC on the surface of the PA-Br1 membrane, the WCA of the PA-PDMC membrane decreases from  $50.0^\circ$  to  $30.6^\circ$  with increasing the ATRP time from 0.2 to 8.0 h. When ATRP time is more than 1.0 h, the WCA of the PA-PDMC membrane is smaller than that of the PA membrane ( $39.0^\circ$ ). Moreover, the surface charge of PA-Br1 and PA-PDMC membranes was evaluated with Zeta potential (Figure 6(b)). The Zeta potential of the PA-Br1 membrane decreases with increasing the pH. The PA-Br1 membrane is positively charged in acid aqueous solutions with low pH due to the adsorption of hydrogen ions. Subsequently, as the pH increases, the carboxylic acid groups of PA-Br1 are deprotonated and hydroxide ions are adsorbed onto the membrane surface in alkaline aqueous solutions, resulting in a negatively charged membrane.<sup>14</sup> After grafting PDMC on the surface of the PA-Br1 membrane, the Zeta potential of the PA-PDMC membrane keeps positively charged. The isoelectric point of the PA-PDMC membrane increases with increasing the ATRP time. In a word, after grafting positively charged PDMC from the surface of the PA-Br1 membrane, the hydrophilicity and surface charge of the PA-PDMC membrane increases with increasing the DMC graft content on the membrane surface.

### Hosted file

image12.emf available at <https://authorea.com/users/469418/articles/562301-chlorine-resistant-positively-charged-nanofiltration-membranes-formed-by-si-atrp-method-for-heavy-metal-ions-removal>

**Figure 6.** (a) Initial water contact angle of PA-Br1 membrane and PA-PDMC membranes grafted via SI-ATRP for different time. (b) Zeta potential varies with pH of PA-Br1 membrane and PA-PDMC membranes grafted via SI-ATRP for different time tested with  $1.0 \text{ mmol L}^{-1}$  KCl aqueous solution at  $25^\circ\text{C}$ .

### 3.3. Separation performance of PA-PDMC membranes.

Apart from Zeta potential, the nanofiltration performance of PA-PDMC membranes for water softening and heavy metal ions removal is associated with the molecular weight cut-off of the membrane. As presented in Figure 7, the molecular weight cut-off of the PA-Br1 membrane is 370 Da. After grafting PDMC on the

surface of the PA-Br1 membrane, the molecular weight cut-off of the PA-PDMC membrane decreases from 350 to 240 Da with increasing the ATRP time from 0.2 to 8.0 h, which is probably ascribed to the increasing selective layer thickness.

**Figure 7.** PEG retention curves of PA-Br1 membrane and PA-PDMC membranes grafted via SI-ATRP for different time tested with 1 g L<sup>-1</sup> PEG aqueous solutions (pH [?]7.0) at 25°C under 0.6 MPa (Insert: molecular weight cut-off of PA-Br1 and PA-PDMCt).

The water flux and solute retentions of PA-PDMC membranes were investigated with water and 1 g L<sup>-1</sup> inorganic salt aqueous solutions. As shown in Figure 8(a), the water flux of the PA-Br1 membrane was 33.0 L m<sup>-2</sup> h<sup>-1</sup>. As the ATRP time increases, the water flux of the PA-PDMC membrane first increased and then decreased (Figure 8(a)). When ATRP time was 0.5 h, the optimum water flux of the PA-PDMC membrane was 102 L m<sup>-2</sup> h<sup>-1</sup>. As the hydrophilicity increased, the water flux of the PA-PDMC membrane increased with increasing the ATRP time from 0.2 to 0.5 h. Subsequently, a decrease in water flux was observed with increasing the ATRP time above 0.5 h. The decrease in water flux was probably attributed to a decrease in molecular weight cut-off of the membrane and the increase in selective layer thickness resulted from high DMC graft content on the membrane surface.

As shown in Figure 8(b), the retentions to Na<sub>2</sub>SO<sub>4</sub>, MgSO<sub>4</sub>, MgCl<sub>2</sub> and NaCl of PA-Br1 membrane were 98.1%, 89.0%, 54.2% and 35.0%, respectively. The retentions of PA-PDMC membranes changed a lot after grafting PDMC from the surface of the PA-Br1 membranes. As far as we know, retentions to inorganic salts of nanofiltration membranes are mainly dominated by the membrane surface charge and molecular weight cut-off (pore size). As the surface charge increased, the retentions to Na<sub>2</sub>SO<sub>4</sub> and MgSO<sub>4</sub> of the PA-PDMC membrane decreased with increasing the ATRP time from 0.2 to 0.5 h. Subsequently, an increase in retentions to Na<sub>2</sub>SO<sub>4</sub> and MgSO<sub>4</sub> was observed with increasing the ATRP time above 0.5 h, which was probably attributed to the decreasing molecular weight cut-off. For the retention of MgCl<sub>2</sub>, these two factors mentioned above are both beneficial to improve retention to MgCl<sub>2</sub>. Consequently, the retention to MgCl<sub>2</sub> increased from 72.0% to 94.9% with the ATRP time increasing from 0.2 to 8.0 h. Unlike the other testing inorganic salts, retention to NaCl was primarily influenced by the molecular weight cut-off of the membrane, and therefore, increased with increasing the ATRP time.

### Hosted file

image15.emf available at <https://authorea.com/users/469418/articles/562301-chlorine-resistant-positively-charged-nanofiltration-membranes-formed-by-si-atrp-method-for-heavy-metal-ions-removal>

**Figure 8.** Separation performance of PA-Br1 and PA-PDMC membranes grafted via SI-ATRP for different time tested with 1 g L<sup>-1</sup> Na<sub>2</sub>SO<sub>4</sub>, MgSO<sub>4</sub>, MgCl<sub>2</sub> and NaCl aqueous solutions (pH [?] 7.0) at 25 °C under 0.6 MPa.

In addition, MgCl<sub>2</sub>, CaCl<sub>2</sub>, CuCl<sub>2</sub>, and ZnCl<sub>2</sub> were used as model inorganic salts to evaluate the performance of PA-PDMC membranes dealing with softening and heavy metal ions removal. As shown in Figure 9, the water flux of the PA-PDMC3 membrane was 82.5 L m<sup>-2</sup>h<sup>-1</sup>. Compared with the PA membrane, the water flux of the PA-PDMC3 membrane was 3.1 times as high as that of the PA membrane. The retentions to MgCl<sub>2</sub>, CaCl<sub>2</sub>, CuCl<sub>2</sub>, and ZnCl<sub>2</sub> of PA-PDMC3 membrane were 92.8%, 90.8%, 93.5% and 96.8%, respectively. Consequently, the PA-PDMC3 membrane exhibited exceptionally higher water flux and retentions to divalent cations than some other positively charged nanofiltration membranes published in recent years (Figure 10).

**Figure 9.** Separation performance of PA, PA-Br1 and PA-PDMC3 membranes tested with 1 g L<sup>-1</sup> MgCl<sub>2</sub>, CaCl<sub>2</sub>, 0.1 g L<sup>-1</sup> CuCl<sub>2</sub>and ZnCl<sub>2</sub> aqueous solutions at 25 °C under 0.6 MPa.

**Figure 10.** Comparative test results of water permeance and MgCl<sub>2</sub> rejection for positively charged nanofiltration membranes published in recent years.<sup>4,21-23,25,40-50</sup>

### 3.4. Stability and chlorine-resistant property of PA-PDMC membranes.

The stability of the membrane is important for the application point of view.<sup>46,51</sup> Therefore, a long-term test of the PA-PDMC membrane was performed with 1 g L<sup>-1</sup>MgCl<sub>2</sub> and 0.1 g L<sup>-1</sup>ZnCl<sub>2</sub> aqueous solution at 25 degC and 0.6 MPa (Figure 11). Both the flux and solute retention to MgCl<sub>2</sub> and ZnCl<sub>2</sub> of the PA-PDMC3 membrane changed little during the long-term run.

### Hosted file

image19.emf available at <https://authorea.com/users/469418/articles/562301-chlorine-resistant-positively-charged-nanofiltration-membranes-formed-by-si-atrp-method-for-heavy-metal-ions-removal>

**Figure 11.** Effect of operation time on water flux and solute retention of PA-PDMC3 membrane tested with 1 g L<sup>-1</sup>MgCl<sub>2</sub> and 0.1 g L<sup>-1</sup>ZnCl<sub>2</sub> at 25 °C and 0.6 MPa.

In the practical separation process, membranes are always exposed to the disinfectant which generally contained active chlorine in the pretreatment process, the ability of chlorine resistance is directly relevant to the lifetime of the membranes.<sup>52,53</sup> To evaluate the chlorine-resistant property of PA-PDMC membrane, the immersion testing method was used.<sup>54,55</sup> The membranes were first immersed in an active chlorine concentration of 100 mg/L NaClO solution for a predetermined time and then tested for nanofiltration performance. As shown in Figure 12, the water flux of the PA-PDMC3 membrane increased by 1.6 times and gradually increased from 82.5 to 136 L m<sup>-2</sup> h<sup>-1</sup> after immersion in 100 mg/L active chlorine solution for 120 h. Meanwhile, the retention to MgCl<sub>2</sub> of the PA-PDMC3 membrane decreased gradually from 92.8% to 82.2%. However, for PEI/TMC polyamide nanofiltration membranes (PEI/TMC, 0.7 wt% PEI aqueous solution, 0.2 wt% TMC hexane solution), the water flux increased by 3.9 times and dramatically increased from 35.3 to 139 L m<sup>-2</sup>h<sup>-1</sup> after immersion in 100 mg/L active chlorine solution just for 2 h. At the same time, the retention of MgCl<sub>2</sub> for PEI/TMC decreased significantly from 93.2% to 70.6%. The chlorine-resistant property of the PA-PDMC membrane demonstrated that the PDMC grafted onto the PA-Br1 membranes can act as a barrier layer to prevent the inner PA layer from being attacked by chlorine directly, while not sacrifice water flux due to the enhancement of hydrophilicity.<sup>30</sup> Consequently, PA-PDMC membrane possessed an exceptional chlorine-resistant property with high permeability and desired rejection of metal ions. In a word, PA-PDMC membrane exhibited exceptional stability and chlorine-resistant property, which had a great potential to deal with softening and heavy metal removal in freshwater production and wastewater purification processing.<sup>3,7</sup>

**Figure 12.** Chlorine resistance of PA-PDMC3 membrane under 100 mg/L active chlorine treatment, including water flux and retention of 1 g L<sup>-1</sup> MgCl<sub>2</sub> aqueous solution.

## 4. CONCLUSIONS

The PA-PDMC membranes with high flux and chlorine resistance were fabricated by grafting DMC on the surface of the PA-Br1 membranes via SI-ATRP. The graft content of PDMC, thickness, and surface charge of the membranes were adjusted by varying the ATRP time. When ATRP time was 3.0 h, the retentions to divalent cations of as-prepared PA-PDMC3 membrane was above 90% with the flux of 82.5 L m<sup>-2</sup>h<sup>-1</sup>. Furthermore, PA-PDMC membranes showed a stable and good separation performance during a long-time filtration process of 168 h and exhibited an exceptional chlorine resistance. Therefore, this work provided a controllable surface modification method to fabricate chlorine-resistant positively charged polyamide nanofiltration membranes for removing heavy metal ions from water.

## ASSOCIATED CONTENT

### AUTHOR INFORMATION

Corresponding Author

\*E-mail: wangnx@bjut.edu.cn; anqf@bjut.edu.cn

Notes

The authors declare no competing financial interest.

## ACKNOWLEDGMENT

This research was financially supported by National Natural Science Foundation of China (No. 21676233, 21878004), Beijing Municipal Natural Science Foundation of co-sponsored by Beijing Natural Science Foundation Committee and Beijing Education Committee (KZ201910005001).

## Reference

1. Kurniawan TA, Chan GYS, Lo WH, Babel S. Physico-chemical treatment techniques for wastewater laden with heavy metals. *Chem Eng J.*2006;118:83-98.
2. Kim S, Chu KH, Al-Hamadani YAJ, et al. Removal of contaminants of emerging concern by membranes in water and wastewater: a review. *Chem Eng J.*2018;335:896-914.
3. Van der Bruggen B, Vandecasteele C. Removal of pollutants from surface water and groundwater by nanofiltration: overview of possible applications in the drinking water industry. *Environ Pollut.*2003;122:435-445.
4. Ye CC, An QF, Wu JK, Zhao FY, Zheng PY, Wang NX. Nanofiltration membranes consisting of quaternized polyelectrolyte complex nanoparticles for heavy metal removal. *Chem Eng J.*2019;359:994-1005.
5. Murthy ZVR, Chaudhari LB. Separation of binary heavy metals from aqueous solutions by nanofiltration and characterization of the membrane using Spiegler-Kedem model. *Chem Eng J.* 2009;150:181-187.
6. Maher A, Sadeghi M, Moheb A. Heavy metal elimination from drinking water using nanofiltration membrane technology and process optimization using response surface methodology. *Desalination.*2014;352:166-173.
7. Petersen RJ. Composite reverse-osmosis and nanofiltration membranes. *J Membr Sci.* 1993;83:81-150.
8. Misdan N, Lau WJ, Ismail AF. Seawater reverse osmosis (SWRO) desalination by thin-film composite membrane-current development, challenges and future prospects. *Desalination.* 2012;287:228-237.
9. Buonomenna MG. Membrane processes for a sustainable industrial growth. *RSC Adv.* 2013;3:5694-5740.
10. Zhao Q, An QF, Ji YL, Qian JW, Gao CJ. Polyelectrolyte complex membranes for pervaporation, nanofiltration and fuel cell applications. *J Membr Sci.*2011;379:19-45.
11. Tang YP, Chan JX, Chung TS, Weber M, Staudt C, Maletzko C. Simultaneously covalent and ionic bridging towards antifouling of GO-imbedded nanocomposite hollow fiber membranes. *J Mater Chem A.*2015;3:10573-10584.
12. Li QL, Mahendra S, Lyon DY, et al. Antimicrobial nanomaterials for water disinfection and microbial control: Potential applications and implications. *Water Res.*2008;42:4591-4602.
13. Fan XC, Dong YN, Su YL, et al. Improved performance of composite nanofiltration membranes by adding calcium chloride in aqueous phase during interfacial polymerization process. *J Membr Sci.*2014;452:90-96.
14. An QF, Sun WD, Zhao Q, Ji YL, Gao CJ. Study on a novel nanofiltration membrane prepared by interfacial polymerization with zwitterionic amine monomers. *J Membr Sci.* 2013;431:171-179.
15. Mi YF, Xu G, Guo YS, Wu B, An QF. Development of antifouling nanofiltration membrane with zwitterionic functionalized monomer for efficient dye/salt selective separation. *J Membr Sci.* 2020;601.
16. Guo YS, Mi YF, Ji YL, An QF, Gao CJ. One-step surface grafting method for preparing zwitterionic nanofiltration membrane via in situ introduction of initiator in interfacial polymerization. *ACS Appl Polym Mater.* 2019;1:1022-1033.
17. Guo YS, Weng XD, Wu B, et al. Construction of nonfouling nanofiltration membrane via introducing uniformly tunable zwitterionic layer. *J Membr Sci.* 2019;583:152-162.

18. Guo YS, Ji YL, Wu B, et al. High-flux zwitterionic nanofiltration membrane constructed by in-situ introduction method for monovalent salt/antibiotics separation. *J Membr Sci.* 2020;593.
19. Peng HW, Zhang WH, Hung WS, et al. Phosphonium modification leads to ultrapermeable antibacterial polyamide composite membranes with unreduced thickness. *Adv Mater.* 2020;32.
20. Simazaki D, Kubota R, Suzuki T, Akiba M, Nishimura T, Kunikane S. Occurrence of selected pharmaceuticals at drinking water purification plants in Japan and implications for human health. *Water Res.*2015;76:187-200.
21. Chiang YC, Hsub YZ, Ruaan RC, Chuang CJ, Tung KL. Nanofiltration membranes synthesized from hyperbranched polyethyleneimine. *J Membr Sci.* 2009;326:19-26.
22. Zhao FY, Ji YL, Weng XD, et al. High-flux positively charged nanocomposite nanofiltration membranes filled with poly(dopamine) modified multiwall carbon nanotubes. *ACS Appl Mater Interfaces.*2016;8:6693-6700.
23. Wang HF, Zhang QF, Zhang SB. Positively charged nanofiltration membrane formed by interfacial polymerization of 3,3',5,5'-biphenyl tetraacyl chloride and piperazine on a poly(acrylonitrile) (PAN) support. *J Membr Sci.*2011;378:243-249.
24. Jaeger W, Bohrisch J, Laschewsky A. Synthetic polymers with quaternary nitrogen atoms Synthesis and structure of the most used type of cationic polyelectrolytes. *Prog Polym Sci.* 2010;35:511-577.
25. Zhu WP, Gao J, Sun SP, Zhang S, Chung TS. Poly(amidoamine) dendrimer (PAMAM) grafted on thin film composite (TFC) nanofiltration (NF) hollow fiber membranes for heavy metal removal. *J Membr Sci.*2015;487:117-126.
26. Lin SS, Huang H, Zeng YJ, Zhang L, Hou LA. Facile surface modification by aldehydes to enhance chlorine resistance of polyamide thin film composite membranes. *J Membr Sci.* 2016;518:40-49.
27. Liu SH, Wu CR, Hou XT, et al. Understanding the chlorination mechanism and the chlorine-induced separation performance evolution of polypiperazine-amide nanofiltration membrane. *J Membr Sci.*2019;573:36-45.
28. Liu MH, Chen Q, Wang LZ, Yu SC, Gao CJ. Improving fouling resistance and chlorine stability of aromatic polyamide thin-film composite RO membrane by surface grafting of polyvinyl alcohol (PVA). *Desalination.* 2015;367:11-20.
29. Huang H, Lin SS, Zhang L, Hou L. Chlorine-resistant polyamide reverse osmosis membrane with monitorable and regenerative sacrificial layers. *ACS Appl Mater Interfaces.* 2017;9:10214-10223.
30. Rana HH, Saha NK, Jewrajka SK, Reddy AVR. Low fouling and improved chlorine resistant thin film composite reverse osmosis membranes by cerium(IV)/polyvinyl alcohol mediated surface modification. *Desalination.* 2015;357:93-103.
31. Rana D, Matsuura T. Surface modifications for antifouling membranes. *Chem Rev.* 2010;110:2448-2471.
32. Yang R, Jang H, Stocker R, Gleason KK. Synergistic prevention of biofouling in seawater desalination by zwitterionic surfaces and low-level chlorination. *Adv Mater.* 2014;26:1711-1718.
33. Chen Z, Xie LY, Huang XY, Li ST, Jiang PK. Achieving large dielectric property improvement in polymer/carbon nanotube composites by engineering the nanotube surface via atom transfer radical polymerization. *Carbon.* 2015;95:895-903.
34. Weng XD, Ji YL, Ma R, Zhao FY, An QF, Gao CJ. Superhydrophilic and antibacterial zwitterionic polyamide nanofiltration membranes for antibiotics separation. *J Membr Sci.* 2016;510:122-130.
35. Yang YF, Li Y, Li QL, Wan LS, Xu ZK. Surface hydrophilization of microporous polypropylene membrane by grafting zwitterionic polymer for anti-biofouling. *J Membr Sci.* 2010;362:255-264.

36. Freger V, Gilron J, Belfer S. TFC polyamide membranes modified by grafting of hydrophilic polymers: an FT-IR/AFM/TEM study. *J Membr Sci.* 2002;209:283-292.
37. Barbey R, Lavanant L, Paripovic D, et al. Polymer brushes via surface-initiated controlled radical polymerization: synthesis, characterization, properties, and applications. *Chem Rev.* 2009;109:5437-5527.
38. Zhao YH, Wee KH, Bai RB. A novel electrolyte-responsive membrane with tunable permeation selectivity for protein purification. *ACS Appl Mater Interfaces.* 2010;2:203-211.
39. Wang JS, Matyjaszewski K. Controlled living radical polymerization-halogen atom-transfer radical polymerization promoted by Cu(I)/Cu(II) redox process. *Macromolecules.* 1995;28:7901-7910.
40. Li XH, Zhang CJ, Zhang SN, Li JX, He BQ, Cui ZY. Preparation and characterization of positively charged polyamide composite nanofiltration hollow fiber membrane for lithium and magnesium separation. *Desalination.* 2015;369:26-36.
41. Lin CE, Fang LF, Du SY, Yao ZK, Zhu BK. A novel positively charged nanofiltration membrane formed via simultaneous cross-linking/quaternization of poly(m-phenylene 5 isophthalamide)/polyethyleneimine blend membrane. *Sep Purif Technol.* 2019;212:101-109.
42. Ma XH, Yang Z, Yao ZK, Xu ZL, Tang CYY. A facile preparation of novel positively charged MOF/chitosan nanofiltration membranes. *J Membr Sci.* 2017;525:269-276.
43. Fang LF, Zhou MY, Cheng L, Zhu BK, Matsuyama H, Zhao SF. Positively charged nanofiltration membrane based on cross-linked polyvinyl chloride copolymer. *J Membr Sci.* 2019;572:28-37.
44. Zhang RN, Su YL, Zhao XT, Li YF, Zhao JJ, Jiang ZY. A novel positively charged composite nanofiltration membrane prepared by bio-inspired adhesion of polydopamine and surface grafting of poly(ethylene imine). *J Membr Sci.* 2014;470:9-17.
45. Zhang QF, Wang HF, Zhang SB, Dai L. Positively charged nanofiltration membrane based on cardo poly(arylene ether sulfone) with pendant tertiary amine groups. *J Membr Sci.* 2011;375:191-197.
46. Ji YL, An QF, Zhao Q, Chen HL, Gao CJ. Preparation of novel positively charged copolymer membranes for nanofiltration. *J Membr Sci.* 2011;376:254-265.
47. Ji YL, An QF, Zhao FY, Gao CJ. Fabrication of chitosan/PDMCHEA blend positively charged membranes with improved mechanical properties and high nanofiltration performances. *Desalination.* 2015;357:8-15.
48. Du RH, Zhao JS. Properties of poly (N,N-dimethylaminoethyl methacrylate)/polysulfone positively charged composite nanofiltration membrane. *J Membr Sci.* 2004;239:183-188.
49. Yan C, Zhang SH, Yang DL, Jian XG. Preparation and characterization of chloromethylated/quaternized poly(phthalazinone ether sulfone ketone) for positively charged nanofiltration membranes. *J Appl Polym Sci.* 2008;107:1809-1816.
50. Huang RH, Chen GH, Sun MK, Gao CJ. Preparation and characterization of quaternized chitosan/poly(acrylonitrile) composite nanofiltration membrane from anhydride mixture cross-linking. *Sep Purif Technol.* 2008;58:393-399.
51. Zhao Q, Ji YL, Wu JK, Shao LL, An QF, Gao CJ. Polyelectrolyte complex nanofiltration membranes: performance modulation via casting solution pH. *RSC Adv.* 2014;4:52808-52814.
52. Shintani T, Matsuyama H, Kurata N. Development of a chlorine-resistant polyamide reverse osmosis membrane. *Desalination.* 2007;207:340-348.
53. Ren PF, Fang Y, Wan LS, Ye XY, Xu ZK. Surface modification of polypropylene microfiltration membrane by grafting poly(sulfobetaine methacrylate) and poly(ethylene glycol): Oxidative stability and antifouling capability. *J Membr Sci.* 2015;492:249-256.

54. Zhao HY, Qiu S, Wu LG, Zhang L, Chen HL, Gao CJ. Improving the performance of polyamide reverse osmosis membrane by incorporation of modified multi-walled carbon nanotubes. *J Membr Sci.*2014;450:249-256.
55. Li W, Lou LY, Hai YY, Fu CX, Zhang JL. Polyamide thin film composite membrane using mixed amines of thiourea and m-phenylenediamine.*RSC Adv.* 2015;5:54125-54132.